View metadata, citation and similar papers at core.ac.uk

brought to you by CORE

provided by Elsevier - Publisher Connector

Deuterium Solid-State NMR Investigations of Exchange Labeled Oriented Purple Membranes at Different Hydration Levels

Burkhard Bechinger* and Martin Weik†

*Max-Planck-Institut für Biochemie, 82152 Martinsried, Germany; and †Laboratoire de Biophysique Moléculaire, Institut de Biologie Structurale, 38027 Grenoble, France

ABSTRACT Oriented purple membranes were equilibrated under controlled ^2H_2O relative humidity ranging from 15% to 93% and introduced into the magnetic field of an NMR spectrometer with the membrane normal parallel to the magnetic field direction. Deuterium solid-state NMR spectra of these samples resolved four deuteron populations. Deuterons that have exchanged with amide protons of the protein exhibited a broad spectral line shape (<150 kHz). Furthermore, a broadened signal of deuterons tightly associated with protein and lipid is detected at low hydration, as well as two additional water populations that were present when the samples were equilibrated at ≥75% relative humidity. These latter ones are characterized by narrow quadrupolar splittings (<2.5 kHz) and orientation-dependent chemical shifts. Their deuterium relaxation times, measured as a function of temperature, indicate correlation times in the fast regime (10^{-10} s) and activation energies of 13 kJ/mol (at 86% relative humidity). Differences in T_1 and T_2 relaxation together with small residual quadrupole splittings show that the mobility of the deuterons is anisotropic. The occurrence of these mobile water populations at high levels of purple membrane hydration (≥75% relative humidity) correlate with proton pumping activity of bacteriorhodopsin, the fast kinetics of M-decay in the bacteriorhodopsin photocycle, and structural alterations of the protein during the M-state, which have been described previously.

INTRODUCTION

The light-driven proton pump bacteriorhodopsin (BR) in the purple membrane (PM) of *Halobacterium salinarum* is one of the best-studied membrane proteins. Absorption of a photon by the light-sensitive chromophore retinal triggers conformational rearrangements and drives the bacteriorhodopsin molecule through a cyclic series of ground state and photointermediates, namely bR, J, K, L, M, N, O, and bR (reviews e.g., Haupts et al., 1999; Lanyi, 1999; Oesterhelt, 1998). The retinal chromophore is attached to the lysine 216 side chain located in helix G of bacterioopsin by means of a Schiff base linkage, thereby separating the cytoplasmic from the extracellular part of the proton channel. The retinal pocket is confined by a flattened ring defined by helices ABCFG. During the photocycle a proton is transferred from the cytoplasmic to the extracellular side of the membrane. The seven transmembrane helical structures of this protein in its ground and intermediate states have been determined to up to 1.55 Å resolution by electron (Grigorieff et al., 1996; Kimura et al., 1997; Subramaniam and Henderson, 2000; Vonck, 2000) and x-ray diffraction techniques using a variety of crystallization conditions (Belrhali et al., 1999; Edman et al., 1999; Essen et al., 1998; Luecke et al., 1999; Royant et al., 2000; Sass et al., 2000). Several water molecules have been detected in the proton translocation pathway (Belrhali et al., 1999; Hauss et al., 1997; Luecke et al., 1998; Luecke, 2000; Papadopoulos et al., 1990; Weik et al., 1998b). Neutron (Dencher et al., 1989; Hauss et al., 1994; Weik et al., 1998b), static (Edman et al., 1999; Luecke et al., 1999; Royant et al., 2000; Sass et al., 2000), and time-resolved x-ray (Koch et al., 1991), as well as electron crystallography experiments (Subramaniam et al., 1999; Subramaniam and Henderson, 2000; Vonck, 1996, 2000) have shown that large conformational alterations of the protein occur during the photocycle. Hydration-dependent alterations in the protein structure and dynamics have been correlated to the slowing of the proton transfer kinetics (Cao et al., 1991; Hauss et al., 1997) and to the conformational rearrangements that occur during the photocycle (Fitter et al., 1998b; Kamikubo et al., 1997; Lehnert et al., 1998; Sass et al., 1997; Weik et al., 1998b).

The M-state consists of at least two substates, namely M_1 and M_2 (Oesterhelt, 1998). Transitions between M-states involve structural changes that are detectable by neutron, x-ray, and electron diffraction experiments. The structural transition consists of an outward movement of helix F by 2 Å and an ordering of the cytoplasmic part of helix G (Subramaniam et al., 1993; Vonck, 1996). These conformational changes were suggested to result in an opening of the protein structure at the cytoplasmic side and are paralleled by the additional association of 10–20 water molecules to the purple membrane (Heberle et al., 1993; Koch et al., 1991; Schulenberg et al., 1995; Varo and Lanyi, 1995). A key event in the BR photocycle is a change in accessibility of the Schiff base from the extracellular to the cytoplasmic part of the membrane. This ''reprotonation switch'' has been proposed to take place during the $M_1 \rightarrow M_2$ transition. During the bR to M_1 part of the photocycle the Schiff base is connected to the extracellular side of the membrane to which

Submitted October 22, 2002, and accepted for publication March 12, 2003.

B. Bechinger's present address is Faculté de Chimie, Institut le Bel, 4, rue Blaise Pascal, 67000 Strasbourg, France.

Address reprint requests to Burkhard Bechinger, Tel.: +33 3 90 24 14 96; Fax: +33 3 90 24 14 90; E-mail: bechinger@chimie.u-strasbg.fr.

© 2003 by the Biophysical Society

0006-3495/03/07/361/09 $2.00

it transfers its proton in the L to M_1 transition, whereas it is connected to the cytoplasmic side in the second part of the photocycle from which it is reprotonated in the M_2 to N transition. Deprotonation and reprotonation of the Schiff base have been observed by spectroscopic methods (Korenstein et al., 1978; Oesterhelt, 1998; Varo and Lanyi, 1991). The M_1 to M_2 transition is hydration and temperature dependent, being absent at temperatures <240 K, or at relative humidities <75% (Sass et al., 1997; Weik et al., 1998b), as well as in the surface mutant D38R (Sass et al., 1998).

Structural investigations by diffraction techniques, molecular modeling, optical spectroscopies and mutagenesis have identified amino acid side chains involved in proton translocation (Lanyi, 1999; Oesterhelt, 1998). These are interconnected by a hydrogen bonding network involving several water molecules. The important role of water has become evident in studies that indicate that proton transport stops when the purple membrane is sufficiently dehydrated (Hauss et al., 1997; Sass et al., 1997). Furthermore, large amplitude motions in the pico- to nanosecond timescale have been correlated to the presence of water, the decay of the M-intermediate and thereby the progress of the photocycle (Ferrand et al., 1993; Fitter et al., 1998b; Fitter et al., 1999; Lehnert et al., 1998). Although the resolution of the BR structures has considerably improved during the most recent investigations, inherent disorder prevents the determination of the accurate number and the positioning of all water molecules. However, detailed information on the dynamical properties of the protein, lipids, and water as well as the observation of conformational transitions are required for a thorough understanding of the mechanisms and the rate-limiting factors of proton transport.

Water that is associated with proteins (Kuntz and Kauzmann, 1974; Rupley and Careri, 1991, and literature cited therein) or with phospholipid membranes (Bechinger and Seelig, 1991; Borle and Seelig, 1983; Finer, 1973; Volke et al., 1994; Wieslander et al., 1978) has previously been studied by NMR spectroscopy. Deuterium solid-state NMR spectroscopy has proven particularly valuable in determining the amount of water associated with macromolecules, its reorientational and exchange dynamics as well as the presence of water layers that differ in their strength of association (Finer, 1973; Peemoeller et al., 1986; Usha and Wittebort, 1989; Volke et al., 1994).

NMR spectroscopic approaches have also been used to record structural details of retinal within the BR binding pocket (Engelhard and Bechinger, 1995; Glaubitz et al., 1999; Helmle et al., 2000; Patzelt et al., 1997; Patzelt et al., 2002; Spohn and Kimmich, 1983). Furthermore the deuterium exchange spectra of purple membranes (Spohn and Kimmich, 1983) or the diffusion rate of water parallel to the purple membrane surface has been measured using NMR techniques (Lechner et al., 1994). NMR investigations of ^2H_2O associated with purple membranes, therefore, provide complementary information to previous studies using diffraction techniques or FTIR spectroscopic approaches (Fitter et al., 1999; Papadopoulos et al., 1990; Pebay-Peyroula et al., 1997; Rogan and Zaccai, 1981; Schulenberg et al., 1995; Spohn and Kimmich, 1983; Weik et al., 1998b; Zaccai and Gilmore, 1979; Zaccai, 1987). In this study, purple membranes were hydrated with ^2H_2O at different levels and studied by deuterium solid-state NMR spectroscopy. The use of oriented samples increases the spectral resolution making accessible more detailed information on the distribution and the amount of membrane-associated water. In addition, this technique is used to measure the dynamics and exchange properties of water molecules.

MATERIALS AND METHODS

About 4.4 mg of PM per sample were oriented by drying a PM suspension in water (20 mg/ml) on three glass coverslips. This procedure led to an orientation of the membrane fragments parallel to the glass surface with a mosaicity of $\sim 10^\circ$ as measured by neutron diffraction on similarly prepared samples (Weik et al., 1998b). The plates were then equilibrated for several days in ^2H_2O atmosphere first at 100% relative humidity (r.h.) and then at the desired r.h. that was fixed by saturated salt solutions (O'Brien, 1948), i.e., 15% (LiCl), 44% (K_2CO_3), 57% (NaBr), 75% (NaCl), 86% (KCl), and 93% (KNO_3). The glass-plate samples were subsequently inserted into tubes (7 mm in diameter), sealed, and introduced into the NMR coil of a commercial double resonance probe head of Bruker AMX/MSL400 or DSX400 solid-state NMR spectrometers. For each sample, tuning and matching of the NMR probe was optimized independently. If not indicated otherwise, the orientation of the membrane normal was parallel to the magnetic field direction. ^2H solid-state NMR spectra of exchange labeled PM and associated water was recorded using a quadrupolar pulse echo sequence (Davis et al., 1976). T_2 values were determined by analyzing the signal intensities as a function of the interpulse delays. T_1 experiments were performed using an inversion-recovery quadrupolar-echo pulse sequence. The resulting relaxation decay data were analyzed using the Bruker XWINNMR software. Either peak intensities or integrals of areas of 3–4 selected regions of the spectrum have been extracted from the spectra in a time-dependent manner. Thereafter the program iterates equations of the type $I = I_o + P \times \exp(-t/T_1)$ or $I = I_o \times \exp(-t/T_2)$ to fit to the experimental I-t parameters. One, two, or three component fits have been performed for each data set. Unless otherwise indicated in the text, one component data fits provided satisfactory results ($SD/I_o \leq 7\%$; SD = standard deviation) and were used for further analysis. Typical experimental parameters were: pulse width 2.4–3.6 μs, interpulse delay 40 μs, recycle delay 500 ms, and 4096 number of scans (15,300 acquisitions for the 15% r.h. samples). Initially, spectra covering a broad spectral width were recorded by setting the dwell time to 1 μs and acquiring $\geq$8 K data points. These data sets were either analyzed to obtain an overview of the full spectral range (exponential line broadening 3000 Hz), or of the central part of the spectrum in detail (line broadening 50 Hz). Later, when only the central portion of the spectra was of interest smaller data sets were recorded (spectral width 50 kHz, dwell time 10 μs, 2 K data points). The temperature of the sample was controlled with a stream of air. Spectra were referenced with respect to ^2H_2O diluted in ^1H_2O. This reference sample was prepared in the following manner: 10 μl ^2H_2O (>98%, Campro, Berlin, Germany) were added into the dry sample tube and the exact amount of water determined gravimetrically. The sample tube was then completely filled with 650 μl double-distilled water and sealed.

RESULTS

Deuterium NMR spectra of oriented PM samples equilibrated in ^2H_2O atmospheres have been recorded and provide

increased resolution when compared to powder pattern samples. The quadrupolar splittings and chemical shifts of these spectra are dependent on the alignment of the molecules with respect to the magnetic field direction. Fig. 1, *A–G*, show ^{2}H-NMR spectra of oriented purple membranes equilibrated in ^2H_2O atmospheres at relative humidities between 93% and 15%. The integrated signal intensities of purple membrane-associated water were determined by comparison with those of a weighted amount of ^2H_2O which was diluted in ^1H_2O. The membrane-associated water signals were further characterized by their chemical shift, their quadrupolar splittings ($\Delta\nu_Q$) as well as their relaxation behavior.

Approximately 0.7–2.5 μmol of ^{2}H-isotope are associated with 1 mg of purple membranes when these are equilibrated at 15% r.h.. As the purple membrane is composed of ~75 wt % BR and 25 wt % lipid (Grigorieff et al., 1996; Kates et al., 1982), this amount of ^{2}H, therefore, corresponds to ~50 deuterons per BR monomer (Fig. 2). Whereas most of this signal intensity is associated with a broad spectral component ($\Delta\nu_Q \leq 150$ kHz, Fig. 1 *G*, cf. below), 20–40% are associated with the ''roof-like'' peak in the central region of the spectrum (-30 kHz $< \nu < 30$ kHz). In the following we will concentrate on this central portion of the NMR spectra. The spectrum of samples obtained at ≤57% r.h. is a composite from many different deuterons, which exhibit anisotropic averaging. The spectral line shape and additional structure within these spectra suggests that the rates and the relative directions of the axes, which both characterize these motions, are not uniform throughout the sample (Fig. 1, *D–F*). The measured integral of the central ^{2}H intensity increases when the relative humidity is augmented from 15% to 93% (Fig. 2). The amount of PM-associated deuterons

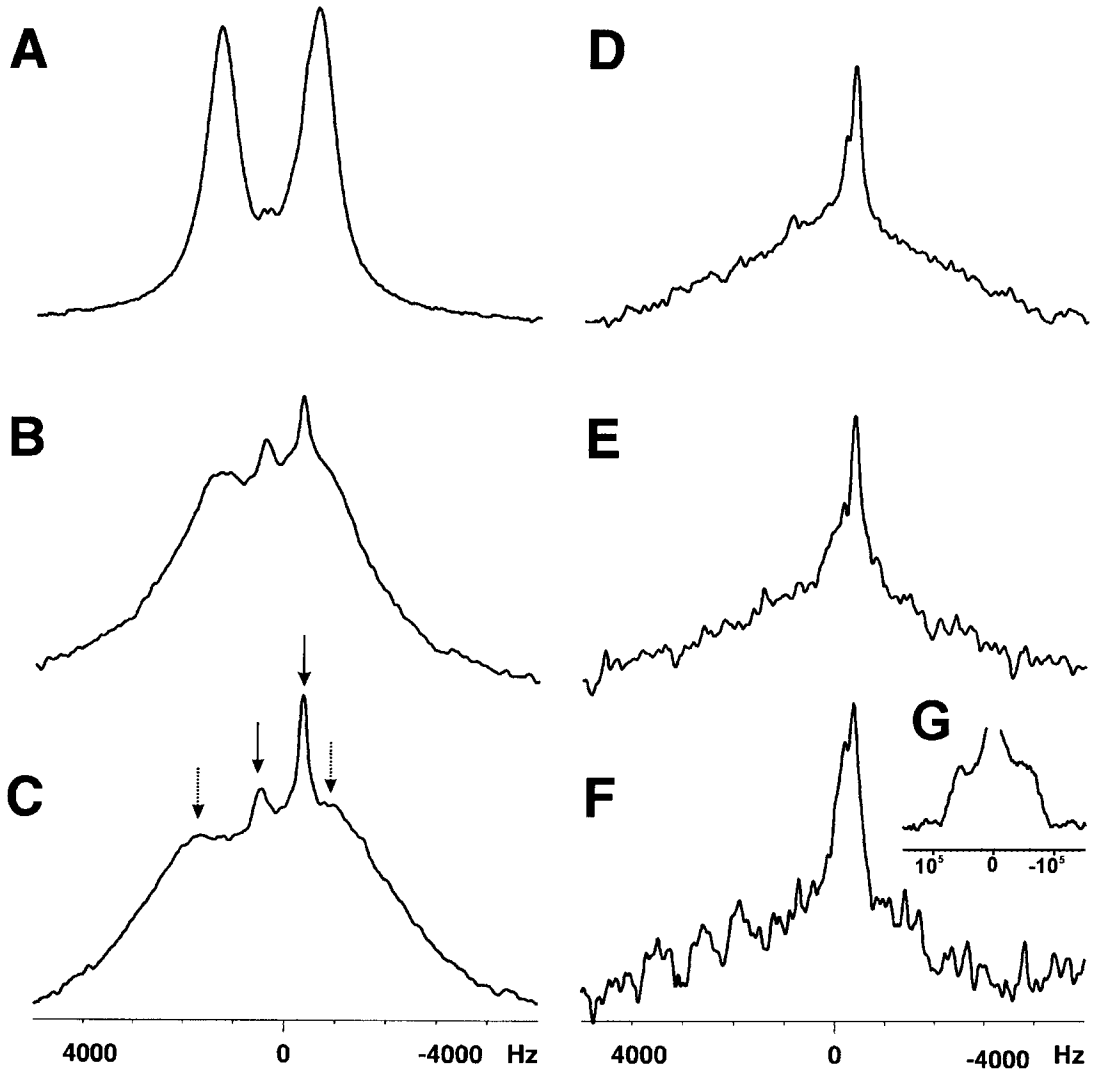

FIGURE 1 Deuterium NMR spectra of purple membranes oriented with their normal parallel to the magnetic field direction and equilibrated over saturated salt solutions in ^2H_2O resulting at the following relative humidity: (*A*) 93%; (*B*) 86%; (*C*) 75% (the dotted and solid arrows point to the peaks defining the large and small quadrupolar splitting, respectively); (*D*) 57%; (*E*) 44%; (*F*) 15%; (*G*) 15% (a spectral window of 250 kHz is shown). The deuterium chemical shift was calibrated relative to the isotropic signal of external ^2H_2O (diluted in ^1H_2O). The spectra were recorded at room temperature.

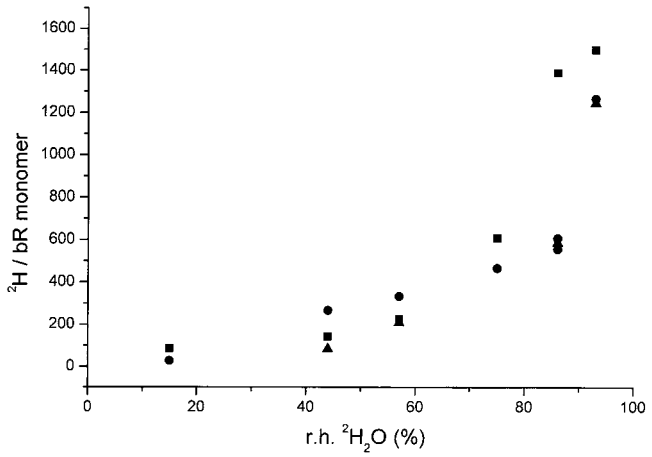

FIGURE 2 The integrated intensities of the central ^{2}H signals obtained at ambient temperature from purple membranes equilibrated over saturated salt solutions in ^2H_2O are shown as a function of vapor pressure: (*circles*) after a few days of equilibration at room temperature; (*triangles*) after storage at 4–10°C for several months; and (*squares*) after reequilibration for two more weeks. The variations between different data sets are due to experimental errors but also due to slow exchange of some of the protons. Different rates of exchange increase the difficulties associated with separating the underlying broad deuterium line shape (cf. Fig. 1 *G*) in a consistent manner from mobile water deuterons.

detected by ^{2}H-NMR (Fig. 2) is in agreement with that determined by comparing the weight of samples when dried over silica gels or when equilibrated at defined humidity (Lehnert et al., 1998).

When the relative humidity is increased ≥75%, a sharp increase in hydration correlates with significant changes in the appearance of the ^{2}H line shapes (Figs. 1, *A–C*, and 2). In addition to the signal already observed at low hydration (maximum at −4 ppm, Fig. 1, *D–G*), intensities with quadrupolar splittings indicative of averaging around an axis that is close to parallel to the membrane normal appear (Fig. 1, *A–C*). The first line exhibits a quadrupolar splitting of 700–800 Hz and a ^{2}H chemical shift of 0.5 ± 1 ppm (Fig. 1, *B* and *C*; orientation of the membrane normal parallel to the magnetic field direction). The second line exhibits a larger quadrupolar splitting and increases strongly in intensity when the hydration of the sample is augmented to 93% r.h. (Fig. 1 *A*). The exact quadrupolar splitting of both resonances is dependent on the degree of hydration and for the latter varies between 1.7 and 2.3 kHz, at relative humidities between 93 and 75%. The anisotropic chemical shift of this resonance is at 5 ± 1.5 ppm. The two quadrupolar doublets newly occurring at 75% r.h. are well separated from each other indicating that exchange between the water populations is slow on the NMR timescale (10^{-3} s). Deconvolution of the spectra shown in Fig. 1, *B* and *C*, indicates that at 86 or 75% r.h. 5–10% of the signal intensities are associated with the line exhibiting a quadrupolar splitting around 800 Hz.

When the sample that has been equilibrated at 86% r.h. is rotated from 0 to 90° in a stepwise manner the anisotropic chemical shift values gradually change from 5 to −4 ppm and from 0.5 to −4.5 ppm, respectively, and the quadrupolar splitting vary in an orientation-dependent manner (Fig. 3). At the same time the resolution of the different water resonances is degraded. The spectra shown in Fig. 3 illustrate the anisotropic nature of the deuterium quadrupole interaction.

The static quadrupolar coupling constant, e^2qQ/h, of ice is ~230 kHz (Bersohn, 1960), therefore, depending on the molecular orientation and dynamics, the quadrupolar couplings range from −170 kHz to 345 kHz. The small quadrupolar splittings observed in samples at relative humidities ≥75% together with the measured correlation times (cf. below) indicate that the water molecules undergo fast reorientation with only a small anisotropic contribution remaining (Fig. 1, *A–C*). In addition to these mobile deuterons, a fourth ^{2}H spectral component (see next paragraph), which exhibits a line width of 120–150 kHz, is detected when the NMR excitation and detection cover a sufficiently large spec-

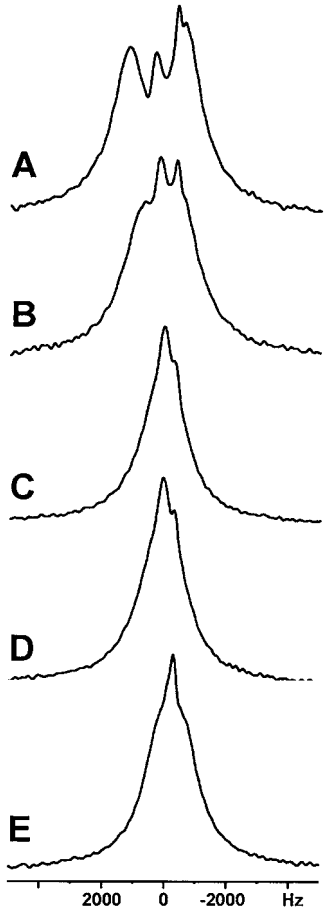

FIGURE 3 ^{2}H-NMR spectra of oriented purple membranes equilibrated over saturated KCl in ^2H_2O (86% r.h.) as a function of tilt angle. The angle between the glass plate normal and the magnetic field direction was adjusted by eye to be approximately: (*A*) 0°; (*B*) 30°; (*C*) 45°; (*D*) 60°; and (*E*) 90°. The spectra were recorded at room temperature.

tral width (Fig. 1 *G*). These broad resonances have been observed previously in lyophilized PM and assigned to amide deuterons that have exchanged during the prolonged incubation of the purple membranes in the ^2H_2O atmosphere (Spohn and Kimmich, 1983).

In summary, four distinct deuteron populations were resolved in Fig. 1. Apart from this broad contribution (Fig. 1 *G*; $\Delta\nu_Q = 120$–150 kHz; relative intensity at 15% r.h. is 0.6–0.8), three other ^2H populations have been distinguished at orientations of the membrane normal parallel to the magnetic field direction: First, $\Delta\nu_Q = 700$–800 Hz and ^2H chemical shift 0.5 ± 1 ppm (Fig. 1, *B* and *C*). Second, $\Delta\nu_Q = 1.7$–2.3 kHz (at r.h. between 93 and 75%) and ^2H chemical shift 5 ± 1.5 ppm (Fig. 1, *A–C*; at 86 or 75% r.h.; the relative intensity of the first when compared to the second contribution is 0.05–0.10). Third, a ''roof-like'' intensity, best visible at r.h. <75% (Fig. 1, *D–F*; relative intensity at 15% r.h. is 0.2–0.4).

Cooling samples which had been equilibrated at 86% r.h. results in the stepwise immobilization of the water molecules and a concomitant disappearance of the motionally averaged NMR signals in the central region of the NMR spectra (Fig. 4). Whereas at temperatures <280 K the lines associated with the 2-kHz signal broaden beyond detection within the ±5 kHz spectral window shown in Fig. 4, the lines associated with the 800-Hz quadrupolar splitting disappear at temperatures <270 K. At 265 K, the remaining spectrum consist of a broad line with a peak at −3 ppm (Fig. 4), thereby resembling the deuterium spectra at low hydration (Fig. 1, *D–F*).

The dynamics of the exchangeable proton and water phases of two samples were further investigated by measuring deuterium relaxation times at 15% and 86% r.h.. At room temperature the deuterium NMR line (measured at 60 MHz) of the sample equilibrated at 86% r.h. exhibits T_2 relaxation times of (174 ± 10) μs and T_1 relaxation times of (12 ± 2) ms. The temperature dependence of T_1 indicates that the water molecules follow the fast correlation time regime (Fig. 5). The T_1 relaxation time is indicative of the presence of correlation times in the 10^{-10} s range; its temperature dependence indicates activation energies of 13 kJ/mol (Fig. 5).

The apparent relaxation times of the sample equilibrated at 15% r.h. are $T_1 = 20$–30 ms and $T_2 = 80$–100 μs. For this sample an improved line fit is obtained when the recycle delay is increased to 7 s and a second slowly relaxing component with ~1/3 of the total intensity is taken into consideration during T_1 analysis. The two-component analysis of the central peak yields T_1 relaxation times of 11 ms and ~1 s (24 ms and ~1 s for the flanking regions). Notably, such slowly relaxing deuterons ($T_1 \gg 100$ ms) cannot exhibit their full signal intensity in spin-counting experiments (Fig. 2). During the line-fitting procedure, average relaxation times have been calculated for both samples although the deuterons are located in different environments. This approach was necessary as most deuterons are expected to exchange with each other and the line shape does not allow for resolving single components. When different parts of the line (center and two neighboring regions) are analyzed independently, the resulting relaxation rates closely resemble each other.

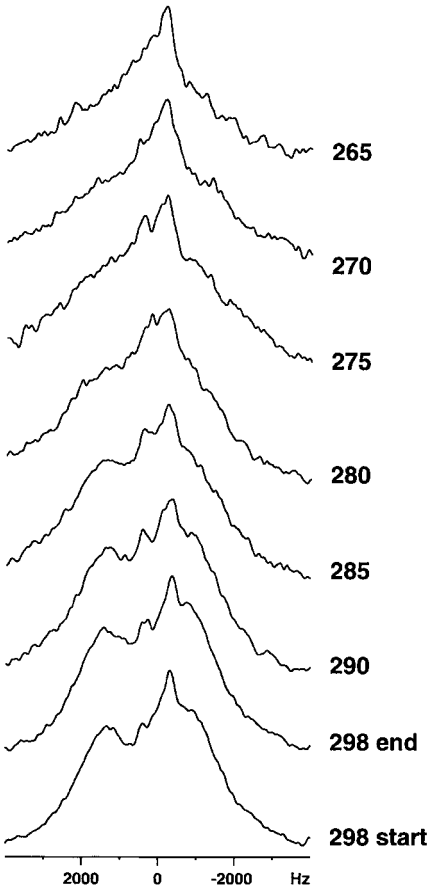

FIGURE 4 ^2H-NMR spectra of purple membranes equilibrated over saturated KCl in ^2H_2O (86% r.h.) and oriented with their normal parallel to the magnetic field direction as a function of temperature (cf. Fig. 1 *B*). The room temperature spectrum at 298 K was recorded in the beginning and at the end of the experiment.

DISCUSSION

Several signals have been resolved in ^2H-NMR spectra of oriented purple membranes, the relative intensities of which depend strongly on the hydration level of the membranes. To assign these signals to different deuteron and water populations within PM comparison with observations by other experiments is useful. At 15% r.h. only PM-associated water that is tightly bound to either BR or purple membrane lipids remains (10 lipids per protein molecule, Essen et al., 1998; Grigorieff et al., 1996; Weik et al., 1998a). The amino acid composition of BR indicates that ≤377 hydrogens potentially exchange with deuterons (247 backbone NH, 129 protons at the side chains and termini and one Schiff base). In addition, exchangeable protons of PM glycolipids (Weik

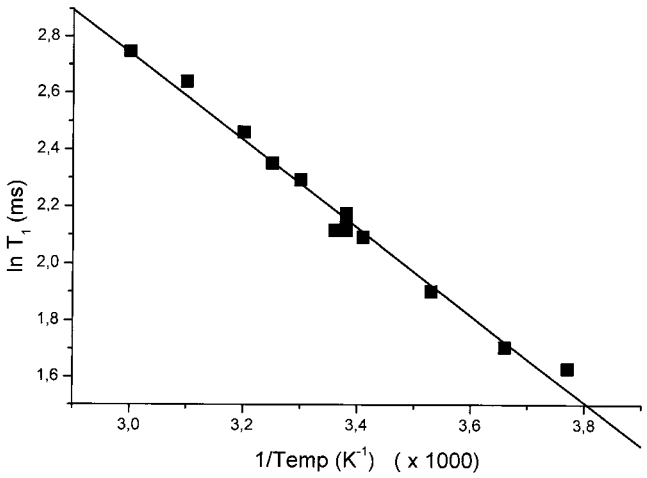

FIGURE 5 Arrhenius plot of the deuterium solid-state NMR T_1 relaxation time of purple membranes equilibrated over saturated KCl in ^2H_2O (86% r.h.).

et al., 1998a) as well as several water molecules that remain associated with the BR pore at 15% r.h. have to be considered (Hauss et al., 1997; Papadopoulos et al., 1990). Changes in the absolute signal intensity, even after several days of equilibration (Fig. 2), suggest that not all of them are easily accessible. This is in agreement with previous infrared spectroscopic investigations where even at full hydration 71% of the BR amide groups remain inexchangeable (Downer et al., 1986).

^{1}H-^{2}H exchange of the amide hydrogens in gramicidin A or lyophilized PM results in solid-state ^{2}H-NMR spectra that are characterized by deuterium quadrupolar splittings $\leq$150 kHz (Datema et al., 1986; Davis, 1988; Spohn and Kimmich, 1983), suggesting that the broad spectral component of hydrated PM samples belongs to hydrogen-bonded deuterons that are associated with the protein backbone or amino acid side chains. Somewhat larger quadrupole splittings have been observed in polycrystalline crambin for which librational motions of the amide ^{2}H-N vector of 8–14° have been calculated (Gosh et al., 1994). In addition, neutron diffraction, FTIR spectroscopy, and molecular modeling experiments indicate that several water molecules are confined within the BR proton channel (Hauss et al., 1997; Papadopoulos et al., 1990; Weik et al., 1998b). These water molecules are tightly bound and some of them can only be removed by exposure of purple membranes to high vacuum (Papadopoulos et al., 1990). Although it has been observed that several water molecules are tightly bound to phospholipid headgroups (Wong and Mantsch, 1988), ^{1}H-^{2}H exchange studied by neutron diffraction indicates that in dry PM samples most hydrogens and water molecules are exchanged at hydrophilic surfaces of the protein (Rogan and Zaccai, 1981).

When the relative humidity is increased to 57% r.h. the amount of membrane-associated water increases (Fig. 2); the ^{2}H-NMR line shape, however, does not exhibit significant alterations (Fig. 1, *D–F*). In the 0–57% r.h. range the lamellar spacing of the membranes remains at a constant value of 49 Å, which corresponds to the membrane thickness (Lechner et al., 1998; Papadopoulos et al., 1990; Weik et al., 1998b). The additional water molecules are, therefore, in tight contact with protein and lipids and do not increase the lamellar spacing.

At 75% r.h. two new populations of water appear, identified by signals with quadrupolar splittings of 0.8 kHz and 2 kHz, and the lamellar spacing of PM is increased to 52 Å (Weik et al., 1998b). Raising the relative humidity further from 75 to 93% leads to addition of ~800 deuterons per BR monomer (Fig. 2) and a concomitant drastic increase in the line exhibiting a quadrupolar splitting of ~2 kHz. Neutron diffraction experiments indicate an increase in the average spacing of PM fragments to 57 Å in the same hydration interval (Lechner et al., 1998). When ^{1}H are exchanged by ^{2}H and the differences recorded by neutron diffraction, it becomes obvious that water does not bind equally to all regions of the PM. Whereas at low r.h. more ^{1}H exchange at protein sites, at 100% r.h. an excess of ~100 molecules per unit cell is observed on areas of the projection map corresponding to lipids (Papadopoulos et al., 1990; Rogan and Zaccai, 1981; Zaccai and Gilmore, 1979). At 47% r.h. the average ^{1}H-^{2}H exchange is about equal for projection areas assigned to protein and lipids (Rogan and Zaccai, 1981). Furthermore, these experiments also indicate that at low hydration additional water is mainly accommodated by expansion of the lipid areas leading to an increase in lateral unit cell dimensions (Rogan and Zaccai, 1981). In contrast, a steep increase in membrane spacing is observed at $\geq$75% r.h. (Lechner et al., 1998; Lehnert et al., 1998; Papadopoulos et al., 1990; Weik et al., 1998b). The emerging deuterium populations in ^{2}H-NMR spectra at relative humidity $\geq$75%, therefore, correlate with the appearance of additional water layers that are loosely bound to purple membranes.

Two water populations are characterized by symmetric ^{2}H-NMR line shapes with quadrupolar splittings of 0.8 and 2 kHz (Fig. 1, *A–C*). Compared to the static quadrupolar coupling constant of ice (230 kHz, Bersohn, 1960), a significant narrowing of the quadrupole splittings to ~0.8 kHz and 2 kHz occurs for PM-associated water indicating fast orientational averaging and exchange of deuterons. Deuterium quadrupole splittings of similar magnitude and asymmetry parameter have been observed when proteins (Borah and Bryant, 1982; Usha and Wittebort, 1989) or pure phospholipid membranes are hydrated with ^2H_2O (Borle and Seelig, 1983; Finer, 1973; Volke et al., 1994).

The ^{2}H-NMR spectra of samples hydrated at 75% or 86% r.h. clearly indicate the existence of two well-separated lines (Fig. 1, *B* and *C*). The presence of a shoulder in the right-hand peak of Fig. 1 *A* suggests that separated lines also exist in the sample hydrated at 93% r.h.. Although fast exchange results in efficient averaging within both water populations,

they exhibit quadrupolar doublets well separated from each other. The two populations differ in their averaged quadrupole splitting and in their ^{2}H chemical shift values.

When changing the relative humidity from 75% r.h. to 93% r.h., an additional 800 deuterons per BR monomer associate with purple membranes (Fig. 2). This value corresponds to an increase of $\sim$0.2 $^2H_2O/Å^2$ and compares reasonably well with the density of water molecules that are part of the hydration shells of liquid crystalline phospholipid membranes (Borle and Seelig, 1983; Faure et al., 1997; Finer, 1973; Volke, 1984). In phospholipid membranes these loosely associated water molecules are in fast exchange with the bulk water phase. Interestingly, in functional and structural studies of the PM the additional water molecules have been shown to be an important determinant of the dynamic properties of the protein-lipid complex (Fitter et al., 1998b; Lehnert et al., 1998).

At 75% r.h. water resonances of $\Delta\nu = 0.8$ kHz and $\Delta\nu = 2$ kHz first appear. When the level of hydration is further increased, the second splitting shows a pronounced increase in intensity (Fig. 1, *A–C*). In comparison, the increase in the first water population remains small. These properties suggest that this latter deuteron population is confined to a limited space, exhibits its own chemical environment, and is well separated from the remaining PM-associated water. Separation of water pools can occur due to continuous protrusions of the protein, or enclosed cavities close to the surface of BR. Alternatively, the 700–800 Hz splitting could be attributed to concealed ^{2}H that are associated, for example, with H-bonded water molecules or exchange-labeled glycolipids. The small quadrupolar splitting observed in Fig. 1, *B* and *C*, represent a few percent of the total ^{2}H-NMR intensity, which is in reasonable agreement with the presence of several phosphoglycerides and glycolipids, including two sulfated triglycosylarcheol lipids located within and between adjacent BR timers in PM (Essen et al., 1998; Weik et al., 1998a).

The water populations appearing at 75% r.h. reorient in the fast correlation time regime and exhibit T_1 and T_2 relaxation times in the 10^{-2} s and 10^{-4} s range, respectively ($\omega = 2\pi \times$ 60 MHz). This dynamic behavior closely parallels the one observed with lysozyme (22 wt % ^2H_2O) and similar models, therefore, apply (Peemoeller et al., 1986). The relaxation times of lysozyme-associated water increase with temperature when analyzed at 5 MHz or 31 MHz indicating that the correlation time τ of the electric field gradient at the site of the ^{2}H nucleus follows the condition $\omega\tau \ll 1$. The water relaxation, however, does not follow a simple fast correlation time regime as $T_1 \gg T_2$. A thorough analysis of the complete data set, under consideration of additional experimental information, suggests that anisotropic averaging of the protein-bound water occurs. Whereas fast rotation ($\tau_f = 10^{-10}$ s) around the direction of the hydrogen bond vector dominates T_1 relaxation, librational movements of this axis ($\tau_s = 10^{-7}$ s) is the main determinant of the T_2 value (Peemoeller et al., 1986). Correlation times of 10^{-10} s have also been deduced from T_1 measurements of crambin-associated water (Usha and Wittebort, 1989) or for the inner hydration shell of phospholipids (Finer, 1973; Volke et al., 1994). This latter water, however, has been shown to be in fast exchange with bulk water ($\tau = 10^{-12}$ s) thereby averaged relaxation and correlation times are observed (Borle and Seelig, 1983; Finer, 1973; Peemoeller et al., 1986; Volke et al., 1994).

The hydration of PM is expected to exert its strongest effect at the loop regions and surface-exposed amino acid side chains. The large effect of the D38R mutation on the photocycle indicates that surface residues might indeed be important for the structural transitions involved in proton pumping (Sass et al., 1998). On the other hand the dynamical behavior of PM is also strongly affected by the degree of its hydration (Ferrand et al., 1993; Fitter et al., 1998b; Lehnert et al., 1998; Zaccai, 1987). Interestingly, when the dynamics in the pico- to nanosecond timescale of PM is probed by neutron scattering experiments an increased ''flexibility'' is observed in fully lipidated and/or ''wet'' membranes (Fitter et al., 1998a). The observed dynamics correlates with proton pumping activity (Fitter et al., 1998b), fast M-decay (Dencher et al., 1999; Hauss et al., 1997; Korenstein and Hess, 1977; Varo and Lanyi, 1995), and conformational rearrangements (Sass et al., 1997; Weik et al., 1998b) that are all only observed at hydration levels $\geq$75% r.h. In contrast, upon progressive dehydration, the ability to complete a full photocycle is more and more reduced and return to the ground state occurs via shunt reactions (Sass et al., 1998). Transitions between M-substates of BR in fully hydrated PM are accompanied by an outward tilt of helix F and a straightening of helix G. These movements result in an opening of the cytoplasmic side of the protein, switching the ion accessibility of the Schiff base from extracellular to cytoplasmic (Oesterhelt, 1998). The volume increase between the bR to M transition corresponds to the binding of 9–20 water molecules (Schulenberg et al., 1995; Varo and Lanyi, 1995). In summary, the results presented indicate that both the structural and the functional transitions correlate with the presence of at least two additional water populations that exhibit fast reorientational correlation times.

We are grateful to Dieter Oesterhelt for the gift of purple membranes. We would also like to acknowledge very valuable comments and discussion contributions by Giuseppe Zaccai.

REFERENCES

Bechinger, B., and J. Seelig. 1991. Conformational changes of the phosphatidylcholine headgroup due to membrane dehydration. A ^{2}H-NMR study. *Chem. Phys. Lipids*. 58:1–5.

Belrhali, H., P. Nollert, A. Royant, C. Menzel, J. P. Rosenbusch, E. M. Landau, and E. Pebay-Peyroula. 1999. Protein, lipid and water organization in bacteriorhodopsin crystals: a molecular view of the purple membrane at 1.9 Angstrom resolution. *Structure Fold Des*. 7:909–917.

Bersohn, R. 1960. Field gradients at the deuterons in molecules. *J. Chem. Phys.* 32:85–88.

Borah, B., and R. G. Bryant. 1982. Deuterium NMR of water in immobilized protein systems. *Biophys. J.* 38:47–52.

Borle, F., and J. Seelig. 1983. Hydration of *Escherichia coli* lipids:deuterium T_1 relaxation time studies of phosphatidylglycerol, phosphatidyethanolamine and phosphatidylcholine. *Biochim. Biophys. Acta.* 735:131–136.

Cao, Y., G. Varo, M. Chan, B. Ni, R. Needleman, and J. K. Lanyi. 1991. Water is required for proton transfer from asparatate-96 to the bacteriorhodopsin Schiff base. *Biochemistry.* 30:10972–10979.

Datema, K. P., K. P. Pauls, and M. Bloom. 1986. Deuterium nuclear magnetic resonance investigation of the exchangeable sites on gramicidin A and gramicidin S in multilamellar vesicles of dipalmitoylphosphatidylcholine. *Biochemistry.* 25:3796–3803.

Davis, J. H. 1988. 2H Nuclear magnetic resonance of exchange-labeled gramicidin in an oriented lyotropic nematic phase. *Biochemistry.* 27:428–436.

Davis, J. H., K. R. Jeffrey, M. Bloom, M. I. Valic, and T. P. Higgs. 1976. Quadrupolar echo deuteron magnetic resonance spectroscopy in ordered hydrocarbon chains. *Chem. Phys. Lett.* 42:390–394.

Dencher, N. A., D. Dresselhaus, G. Zaccai, and G. Buldt. 1989. Structural changes in bacteriorhodopsin during proton translocation revealed by neutron diffraction. *Proc. Natl. Acad. Sci. USA.* 86:7876–7879.

Dencher, N. A., J. Fitter, and R. E. Lechner. 1999. Hydration of biological membranes: role of water in structure, dynamics, and function of the proton pump bacteriorhodopsin. *In* Hydration Processes in Biology. M.-C. Bellissent-Funel, editor. IOS Press, Les Houches, France. 195–217.

Downer, N. W., T. J. Bruchman, and J. H. Hazzard. 1986. Infrared spectroscopic study of photoreceptor membrane and purple membrane. Protein secondary structure and hydrogen deuterium exchange. *J. Biol. Chem.* 261:3640–3647.

Edman, K., P. Nollert, A. Royant, H. Belrhali, E. Pebay-Peyroula, J. Hadju, R. Neutze, and E. Landau. 1999. High-resolution X-ray structure of an early intermediate in the bacteriorhodopsin photocycle. *Nature.* 401:822–826.

Engelhard, M., and B. Bechinger. 1995. Application of NMR-spectroscopy to retinal proteins. *Isr. J. Chem.* 35:273–288.

Essen, L. O., R. Siegert, W. D. Lehmannn, and D. Oesterhelt. 1998. Lipid patches in membrane protein oligomers - crystal structure of the bacteriorhodopsin-lipid complex. *Proc. Natl. Acad. Sci. USA.* 95:11673–11678.

Faure, C., L. Bonakdar, and E. J. Dufourc. 1997. Determination of DMPC hydration in the L_α and L_β phases by ^2H solid state NMR of D_2O. *FEBS Lett.* 405:263–266.

Ferrand, M., A. J. Dianoux, W. Petry, and G. Zaccai. 1993. Thermal motions and function of bacteriorhodopsin in purple membranes: effects of temperature and hydration studied by neutron scattering. *Proc. Natl. Acad. Sci. USA.* 90:9668–9672.

Finer, E. G. 1973. Interpretation of deuterium nuclear magnetic resonance spectroscopic studies of the hydration of macromolecules. *J. Chem. Soc. Faraday Trans. II.* 69:1590–1600.

Fitter, J., O. P. Ernst, T. Hauss, R. E. Lechner, K. P. Hofmann, and N. A. Dencher. 1998a. Molecular motions and hydration of purple membranes and disk membranes studied by neutron scattering. *Eur. Biophys. J.* 27: 638–645.

Fitter, J., R. E. Lechner, and N. Dencher. 1999. Interactions of hyration water and biological membranes studied by neutron scattering. *J. Phys. Chem. B.* 103:8036–8050.

Fitter, J., S. A. Verclas, R. E. Lechner, H. Seelert, and N. A. Dencher. 1998b. Function and picosecond dynamics of bacteriorhodopsin in purple membrane at different lipidation and hydration. *FEBS Lett.* 433:321–325.

Glaubitz, C., I. J. Burnett, G. Gröbner, A. J. Mason, and A. Watts. 1999. Deuterium-MAS NMR spectroscopy on oriented membrane proteins: applications to photointermediates of bacteriorhodopsin. *J. Am. Chem. Soc.* 121:5787–5794.

Gosh, P., S. F. Mel, and R. M. Stroud. 1994. The domain structure of the ion channel-forming protein colicin Ia. *J. Struct. Biol.* 1:597–604.

Grigorieff, N., T. A. Ceska, K. H. Downing, J. M. Baldwin, and R. Henderson. 1996. Electron crystallographic refinement of the structure of bacteriorhodopsin. *J. Mol. Biol.* 259:393–421.

Haupts, U., J. Tittor, and D. Oesterhelt. 1999. Closing in on bacteriorhodopsin: progress in understanding the molecule. *Annu. Rev. Biophys. Biomol. Struct.* 28:367–399.

Hauss, T., G. Büldt, M. P. Heyn, and N. A. Dencher. 1994. Light-induced isomerization causes an increase in the chromophore tilt in the M intermediate of bacteriorhodopsin: a neutron diffraction study. *Proc. Natl. Acad. Sci. USA.* 91:11854–11858.

Hauss, T., G. Papadopoulos, S. A. W. Verclas, G. Büldt, and N. A. Dencher. 1997. Neutron diffraction on purple membranes – essential water molecules in the light-driven proton pump bacteriorhodopsin. *Physica. B.* 234:217–219.

Heberle, J., D. Oesterhelt, and N. A. Dencher. 1993. Decoupling of photo- and proton cycle in the Asp85→Glu mutant of bacteriorhodopsin. *EMBO J.* 12:3721–3727.

Helmle, M., H. Patzelt, W. Gärtner, D. Oesterhelt, and B. Bechinger. 2000. Refinement of the geometry of the retinal binding pocket in dark adapted bacteriorhodopsin by heteronuclear solid-state NMR distance measurements. *Biochemistry.* 39:10066–10071.

Kamikubo, H., T. Oka, Y. Imamoto, F. Tokunaga, J. K. Lanyi, and M. Kataoka. 1997. The last phase of the reprotonation switch in bacteriorhodopsin – the transition between the M-type and the N-type protein conformation depends on hydration. *Biochemistry.* 36:12282–12287.

Kates, M., S. C. Kushawaha, and G. D. Sprott. 1982. Lipids of purple membrane from extreme halophiles and methanogenic bacteria. *Methods Enzymol.* 88:98–111.

Kimura, Y., D. G. Vassylyev, A. Miyazawa, A. Kidera, M. Matsushima, K. Mitsuoka, K. Murata, T. Hirai, and Y. Fujiyoshi. 1997. Surface of bacteriorhodopsin revealed by high-resolution electron crystallography. *Nature.* 389:206–211.

Koch, M. H., N. A. Dencher, D. Oesterhelt, H. J. Plohn, G. Rapp, and G. Buldt. 1991. Time-resolved X-ray diffraction study of structural changes associated with the photocycle of bacteriorhodopsin. *EMBO J.* 10:521–526.

Korenstein, R., and B. Hess. 1977. Hydration effects on the photocycle of bacteriorhodopsin in thin layers of purple membrane. *Nature.* 270:184–186.

Korenstein, R., B. Hess, and B. Kuschmitz. 1978. Branching reactions in the photocycle of bacteriorhodopsin. *FEBS Lett.* 93:266–277.

Kuntz, I. D., Jr., and W. Kauzmann. 1974. Hydration of proteins and polypeptides. *Adv. Protein Chem.* 28:239–345.

Lanyi, J. K. 1999. Bacteriorhodopsin. *Int. Rev. Cytol.* 187:161–202.

Lechner, R. E., N. A. Dencher, J. Fitter, and T. Dippel. 1994. Two-dimensional proton diffusion on purple membrane. *Solid State Ionics.* 70:296–304.

Lechner, R. E., J. Fitter, N. A. Dencher, and T. Hauss. 1998. Dehydration of biological membranes by cooling: an investigation on the purple membrane. *J. Mol. Biol.* 277:593–603.

Lehnert, U., V. Reat, M. Weik, G. Zaccai, and C. Pfister. 1998. Thermal motions in bacteriorhodopsin at different hydration levels studied by neutron scattering: correlation with kinetics and light-induced conformational changes. *Biophys. J.* 75:1945–1952.

Luecke, H. 2000. Atomic resolution structures of bacteriorhodopsin photocycle intermediates: the role of discrete water molecules in the function of this light-driven ion pump. *Biochim. Biophys. Acta.* 1460:133–156.

Luecke, H., H. T. Richter, and J. K. Lanyi. 1998. Proton transfer pathways in bacteriorhodopsin at 2.3 Angstrom resolution. *Science.* 280:1934–1937.

Luecke, H., B. Schobert, H. T. Richter, J. P. Cartailler, and J. K. Lanyi. 1999. Structure of bacteriorhodopsin at 1.55 angstrom resolution. *J. Mol. Biol.* 291:899–911.

O'Brien, F. E. M. 1948. The control of humidity by saturated salt solutions. *J. Sci. Instr.* 25:73–76.

Oesterhelt, D. 1998. The structure and mechanism of the family of retinal proteins from halophilic archaea. *Curr. Opin. Struct. Biol.* 8:489–500.

Papadopoulos, G., N. A. Dencher, G. Zaccai, and G. Buldt. 1990. Water molecules and exchangeable hydrogen ions at the active centre of bacteriorhodopsin localized by neutron diffraction. Elements of the proton pathway? *J. Mol. Biol.* 214:15–19.

Patzelt, H., B. Simon, A. terLaak, B. Kessler, R. Kühne, P. Schmieder, D. Oesterhelt, and H. Oschkinat. 2002. The structures of the active center in dark-adapted bacteriorhodopsin by solution-state NMR spectroscopy. *Proc. Natl. Acad. Sci. U.S.A.* 99:9765–9770.

Patzelt, H., A. S. Ulrich, H. Egbringhoff, P. Dux, J. Ashurst, B. Simon, H. Oschkinat, and D. Oesterhelt. 1997. Towards structural investigations on isotope labelled native bacteriorhodopsin in detergent micelles by solution-state NMR spectroscopy. *J. Biomol. NMR.* 10:95–106.

Pebay-Peyroula, E., G. Rummel, J. P. Rosenbusch, and E. M. Landau. 1997. X-ray structure of bacteriorhodopsin at 2.5 angstroms from microcrystals grown in lipidic cubic phases. *Science.* 277:1676–1681.

Peemoeller, H., F. G. Yeomans, D. W. Kydon, and A. R. Sharp. 1986. Water molecule dynamics in hydrated lysozyme: a deuteron magnetic resonance study. *Biophys. J.* 49:943–948.

Rogan, P. K., and G. Zaccai. 1981. Hydration in purple membrane as a function of relative humidity. *J. Mol. Biol.* 145:281–284.

Royant, A., K. Edman, T. Ursby, E. Pebay-Peyroula, E. Landau, and R. Neutze. 2000. Helix deformation is coupled to vectorial proton trasnport in the photocycle of bacteriorhodopsin. *Nature.* 406:645–648.

Rupley, J. A., and G. Careri. 1991. Protein hydration and function. *Adv. Protein Chem.* 41:37–172.

Sass, H. J., G. Büldt, R. Gessenich, D. Hehn, D. Neff, R. Schlesinger, J. Berendzen, and P. Ormos. 2000. Structural alterations for proton translocation in the M state of wild-type bacteriorhodopsin. *Nature.* 406:649–652.

Sass, H. J., R. Gessenich, M. H. Koch, D. Oesterhelt, N. A. Dencher, G. Buldt, and G. Rapp. 1998. Evidence for charge-controlled conformational changes in the photocycle of bacteriorhodopsin. *Biophys. J.* 75: 399–405.

Sass, H. J., I. W. Schachowa, G. Rapp, M. H. J. Koch, D. Oesterhelt, N. A. Dencher, and G. Büldt. 1997. The tertiary structural changes in bacteriorhodopsin occur between M states: X-ray diffraction and Fourier transform infrared spectroscopy. *EMBO J.* 16:1484–1491.

Schulenberg, P. J., W. Gärtner, and S. E. Braslavsky. 1995. Time-resolved volume changes during the bacteriorhodopsin photo cycle: a photothermal beam deflection study. *J. Phys. Chem.* 99:9617–9624.

Spohn, K. H., and R. Kimmich. 1983. Characterization of the mobility of various chemical groups in the purple membrane of halobacterium halobium by ^{13}C, ^{31}P and ^{2}H solid state NMR. *Biochem. Biophys. Res. Commun.* 114:713–720.

Subramaniam, S., M. Gerstein, D. Oesterhelt, and R. Henderson. 1993. Electron diffraction analysis of structural changes in the photocycle of bacteriorhodopsin. *EMBO J.* 12:1–8.

Subramaniam, S., and R. Henderson. 2000. Molecular mechanism of vectorial proton translocation by bacteriorhodopsin. *Nature.* 406:653–657.

Subramaniam, S., I. Lindahl, P. Bullough, A. R. Faruqi, J. Tittor, D. Oesterhelt, L. Brown, J. Lanyi, and R. Henderson. 1999. Protein conformational changes in the bacteriorhodopsin photocycle. *J. Mol. Biol.* 287:145–161.

Usha, M. G., and R. J. Wittebort. 1989. Orientational ordering and dynamics of the hydrate and exchangeable hydrogen atoms in crystalline crambin. *J. Mol. Biol.* 208:669–678.

Varo, G., and J. K. Lanyi. 1991. Distortions in the photocycle of bacteriorhodopsin at moderate hydration. *Biophys. J.* 59:313–322.

Varo, G., and J. K. Lanyi. 1995. Effects of hydrostatic pressure on the kinetics reveal a volume increase during the bacteriorhodopsin photocycle. *Biochemistry.* 34:12161–12169.

Volke, F. 1984. The orientation dependence of deuterium transverse relaxation rates obtained from unoriented model membrane systems. *Chem. Phys. Lett.* 112:551–554.

Volke, F., S. Eisenblatter, J. Galle, and G. Klose. 1994. Dynamic properties of water at phosphatidylcholine lipid-bilayer surfaces as seen by deuterium and pulsed field gradient proton NMR. *Chem. Phys. Lipids.* 70:121–131.

Vonck, J. 1996. A three-dimensional difference map of the N intermediate in the bacteriorhodopsin photocycle - part of the F helix tilts in the M to N transition. *Biochemistry.* 35:5870–5878.

Vonck, J. 2000. Structure of the bacteriorhodopsin mutant F219L N intermediate revealed by electron crystallography. *EMBO J.* 19:2152–2160.

Weik, M., H. Patzelt, G. Zaccai, and D. Oesterhelt. 1998a. Localization of glycolipids in membranes by in vivo labeling and neutron diffraction. *Mol. Cell.* 1:411–419.

Weik, M., G. Zaccai, N. A. Dencher, D. Oesterhelt, and T. Hauss. 1998b. Structure and hydration of the M-state of the bacteriorhodopsin mutant D96N studied by neutron diffraction. *J. Mol. Biol.* 275:625–634.

Wieslander, A., J. Ulmius, G. Lindblom, and K. Fontell. 1978. Water binding and phase structures for different *Acholeplasma laidlawii* membrane lipids studied by deuteron nuclear magnetic resonance and X-ray diffraction. *Biochim. Biophys. Acta.* 512:241–253.

Wong, P. T. T., and H. H. Mantsch. 1988. High-pressure infrared spectroscopic evidence of water binding sites in 1,2-diacyl phospholipids. *Chem. Phys. Lipids.* 46:213–224.

Zaccai, G. 1987. Structure and function of purple membranes in different conditions. *J. Mol. Biol.* 194:569–572.

Zaccai, G., and D. J. Gilmore. 1979. Areas of hydration in the purple membrane of *Halobacterium halobium*: a neutron diffraction study. *J. Mol. Biol.* 132:181–191.